Energy 70 (2014) 58–67

Contents lists available at ScienceDirect

Energy

journal homepage: www.elsevier.com/locate/energy

# Torrefaction modelling for lignocellulosic biomass conversion processes

Emanuela Peduzzi [a,b,*], Guillaume Boissonnet [a], Geert Haarlemmer [a], Capucine Dupont [a], François Maréchal [b]

[a] Commissariat à l'Energie Atomique et aux Energies Alternatives, LITEN/DTBH/SBRT/Biomass Technology Laboratory, 17 rue des Martyrs, 38054 Grenoble Cedex 9, France
[b] Ecole Polytechnique Fédérale de Lausanne, Industrial Process and Energy Systems Engineering, Station postale 9, 1015 Lausanne, Switzerland

## ARTICLE INFO

*Article history:*
Received 16 January 2014
Received in revised form
17 March 2014
Accepted 21 March 2014
Available online 16 April 2014

*Keywords:*
Torrefaction
Biomass
Process modelling

## ABSTRACT

The objective of this study is to develop a model for the description of torrefaction. The model is conceived in the context of process modelling and therefore it aims at providing coherent mass and energy balances of solid and gaseous products, rather than a physical description of the process. The rationale underlying the proposed model stems from the representation of torrefaction and its products on a C–H–O ternary diagram and its focus is the description of the solid product in terms of yield, composition and heating value. The heating value of the gaseous products is determined by considering water, carbon dioxide and acetic acid as the major volatile products and closing the mass balance. It is possible to extend the number of species considered in the torrefaction gases if experimental data regarding the volatile products are available. The proposed model is simple, of easy implementation and calibration, of fast resolution and its results have been validated against experimental data. This work represents the basis for a future evaluation and optimisation of torrefaction as a pretreatment step in the thermo-chemical conversion of biomass.

© 2014 Elsevier Ltd. All rights reserved.

## 1. Introduction

Torrefaction is a thermo-chemical process generally carried out in the 200–300 °C temperature range, at low heating rates ($<50$ °C/min), and relatively long reaction times (about 1 h) [1]. It may be used as a pre-treatment technology to upgrade lignocellulosic biomass to a higher quality fuel, for its subsequent conversion into heat or other energy carriers, such as electricity and biofuels.

During torrefaction biomass is completely dried and its hygroscopic nature is at least partly lost (only 1 to 6$\%_{wt}$ moisture may be regained) [1] and microbial activity is reduced [2]. The torrefied solid, compared to raw biomass, exhibits better grindability [3,4] and better transport properties for injection (in a boiler or gasifier, for example). Energy content of torrefied biomass is higher while ignition times are shorter [5]. These features make torrefied biomass similar to coal and therefore suitable for co-firing and gasification, with minimal efficiency loss even in existing equipment designed for coal [6]. Furthermore because of the improved storage properties and the higher energy density, transportation costs may be reduced with the production of high quality pellets [6].

This study presents a simple torrefaction model to estimate the solid and gaseous yields, and their corresponding heating values. The results of the model are compared to experimental values obtained in previous studies at CEA Grenoble (Commissariat à l'énergie atomique et aux énergies alternatives) and the literature. The model is implemented in a flow sheeting software (Vali by Belsim [7]), in order to estimate the complete mass and energy balances of a torrefaction unit. This includes the combustion of the off-gases used to provide at least part of the heating requirement of the process.

Torrefaction has a high potential of becoming a leading pre-treatment technology for the efficient exploitation of biomass for energy purposes. It has gained increasing attention from both industry and research institutions in terms of a deeper understanding of the fundamental reaction mechanisms and the engineering of novel reactor designs.

---

* Corresponding author. Commissariat à l'Energie Atomique et aux Energies Alternatives, LITEN/DTBH/SBRT/Biomass Technology Laboratory, 17 rue des Martyrs, 38054 Grenoble Cedex 9, France.
*E-mail address:* emanuela.peduzzi@epfl.ch (E. Peduzzi).

http://dx.doi.org/10.1016/j.energy.2014.03.086
0360-5442/© 2014 Elsevier Ltd. All rights reserved.

**Acronyms**

| | |
|---|---|
| AWL | anhydric weight loss |
| LHV | lower heating value |
| HHV | higher heating value |
| FTIR | Fourier transform infrared spectroscopy |

*List of symbols*

| | |
|---|---|
| B00 | biomass, 0% moisture |
| $c_p$ | heat capacity, kJ $kg^{-1}$ $K^{-1}$ |
| $E_A$ | activation energy, J $mol^{-1}$ |
| $\Phi$ | humidity, $kg_{H_2O}.kg_{tot}^{-1}$ |
| $\Delta_f H°$ | standard enthalpy of formation, kJ/mol |
| $k$ | reaction rate, $s^{-1}$ |
| $\dot{m}$ | mass flow, kg $s^{-1}$ |
| $T$ | Temperature, °C or K |
| T00 | torrefied biomass, 0% moisture |

## 2. Review of torrefaction

The products of torrefaction are a brown/dark coloured solid, permanent gases and condensable species as summarized in Fig. 1 by Bergman [1].

The solid product displays decreasing hydrogen to carbon (H/C) and oxygen to carbon (O/C) elemental ratios that tend towards those of coal with increasing severity of torrefaction (the severity of torrefaction is the degree of conversion and increases with temperature and reaction time). Torrefaction products may be classified differently according to different authors. Here, as a reference, the definition given by Bergman [1] is adopted, as displayed in Fig. 1. According to Bergman *permanent* gases are $H_2$, CO, $CO_2$, $CH_4$ (compounds with a boiling point below −33 °C) and light aromatics such as benzene and toluene. The *condensable* products include three subgroups: water, lipids and organics. Water is a product of thermal decomposition and evaporation of residual moisture. Lipids and organics, usually referred to as *extractable* species, are present in the original biomass and are partly released during torrefaction [8]. Organics may be also produced during devolatilisation and carbonisation [1]. The solid yield, the type and amount of gases produced strongly depend on the operating conditions and also the initial biomass type [1,9]. A review of the numerous *condensable* and permanent gases identified during torrefaction is provided by Tumuluru et al. [9].

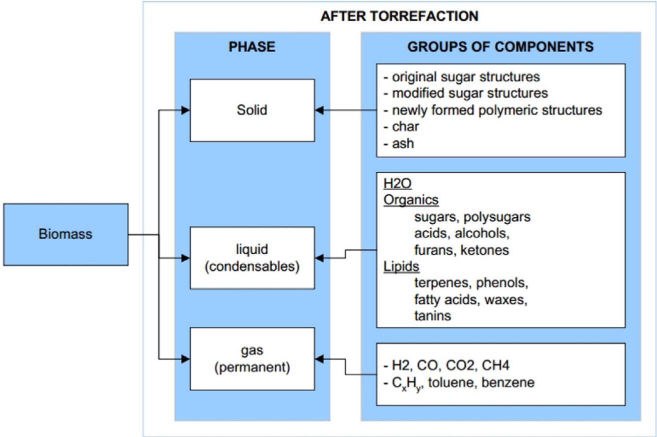

**Fig. 1.** Products of torrefaction, after Bergman [1].

Very few models proposed in the literature for the process modelling of torrefaction take into account the solid and gaseous yields, and their composition as a function of the operating conditions. Models used in techno-economic evaluations are generally relative to a single operating point (in terms of biomass composition, AWL (anhydric weight loss), and temperature) and therefore are represented by a single equation. Hall [10] fit a quadratic regression to relate the AWL occurring during torrefaction and temperature, while they consider constant fractions of volatiles based on experimental results. The model proposed by Medic et al. [11] also uses quadratic regressions to relate the AWL and the energy yield to temperature and moisture content. The models based on empirical correlations, obtained under specific experimental conditions, do not describe the composition of the torrefied solid and evolution of the torrefaction gases during torrefaction. An interesting and complete model describing the solid and gaseous yields as a function of temperature and residence time is proposed by Bates and Ghoniem [12], which is calibrated on the volatiles produced by torrefaction of willow and experimentally measured by Prins et al. [13,14]. These models are generally independent from the torrefaction process design, as they do not take into account the reactor technology, and heat and mass transfer mechanisms at the reactor scale.

Torrefaction reactors are generally classified into two broad categories based on the heat transfer mechanism: direct and indirect heating. For directly heated reactors biomass is in direct contact with the heating media which may be hot gas, hot solids, superheated steam (microwave reactors also fall in this category). For indirectly heated torrefiers biomass is heated across the reactor walls. Different types of torrefaction reactors are reviewed by Dhungana et al. [6] and by Chew and Doshi [15].

## 3. Torrefaction on a ternary diagram

Ternary diagrams are often used in the literature to represent organic chemical processes. Cairns and Tevebaugh [16] introduced the use of C–H–O ternary diagrams to represent carbon deposition boundaries for fuel cell applications. Prins et al. [17] used ternary diagrams to analyse the efficiency of gasification of wood and torrefied wood while Ptasinski et al. [18] used them to compare the gasification of different biofuels and coal. More recently Tay et al. [19] used ternary diagrams to develop a graphical targeting tool for the optimisation of gasification as a function of downstream process requirements, in the context of syngas based integrated biorefineries. Chen et al. [20] used ternary diagrams to describe the solid and gas products composition versus operating conditions during pyrolysis. In the present study the representation of biomass and torrefaction products on a carbon–hydrogen–oxygen (C–H–O) ternary diagram underlies the rationale for the proposed torrefaction model.

The data obtained by Nocquet [8,21,22] are used here for representation purposes as they provide both the solid and gaseous yields obtained during torrefaction. The study was carried out using the lab-scale reactor TORNADE, developed at CEA Grenoble and described in detail in Refs. [8,21,22]. Samples of 100–200 mg of beech wood are torrefied, under $N_2$ flow, at torrefaction temperatures ranging from 220 °C to 300 °C in the isothermal zone of a furnace. The gaseous products are measured on-line by FTIR (Fourier transform infrared spectroscopy) at 150 °C to avoid condensation. Condensable species are collected in two cooling baths: the first one containing freezing ice (wall temperature of 0 °C) and the second one containing frozen carbon dioxide mixed with isopropanol (wall temperature of −70 °C). The eight main species measured were: water, formaldehyde, acetic acid, and carbon dioxide with smaller amounts of carbon monoxide, methanol, formic acid and furfural. These eight measured species combined account together for over 70% of the total volatiles

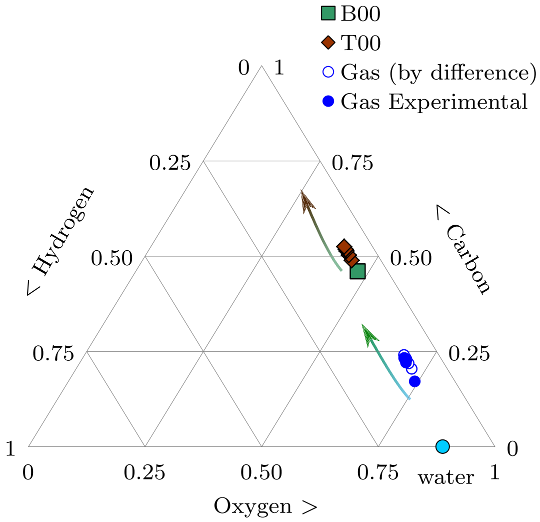

**Fig. 2.** Ternary diagram representing the average composition of biomass and torrefaction solid and gaseous products. Torrefaction is carried out at 280 °C and the values of AWL vary from 0.10 to 0.30. The arrows indicate the evolution of the composition with increasing values of AWL. Data adapted from the work by Nocquet [8,21].

produced. The overall mass balance is closed between 97% and 104% [8,21].

Hereafter the products of torrefaction are considered to be only *gaseous* products and *solid* products and no distinction is made between permanent (gases) and condensable (liquids) described in Fig. 1. Fig. 2 presents on a ternary diagram the average carbon, hydrogen, oxygen mass fractions obtained by Nocquet for the torrefaction of beech wood at 280 °C. The arrows indicate the direction of evolution of the average composition of torrefaction solid and gases[1] as the reaction time, and consequently the AWL, increase. From the initial biomass composition the torrefied solid (brown circles) displays an increasing concentration in carbon, and decreasing concentration in oxygen and hydrogen, as expected. Relying on this result it is possible to infer that the average composition of the torrefaction gases follows a similar trend. This is displayed in Fig. 2 by the empty blue (in web version) circles representing the average composition of the difference between initial biomass and solid torrefaction product. The corresponding experimental results, represented with the filled blue circles, follow the same trend. The difference between the inferred and experimental average gas composition may be ascribed to the difficulty in accurately identifying and quantifying torrefaction gases and, to a lesser extent, to the error relative to the determination of the solid biomass composition. Fig. 2 shows that the average composition of torrefaction gases may be represented on a ternary diagram in a direction that evolves roughly from the average composition of water to that of the initial biomass.

## 4. Torrefaction model

The objective of this study is to propose a simple model for the process modelling of torrefaction, taking into account the solid and gaseous composition and energy yield, as a function of the operating conditions. The model proposed by Bates and Ghoniem [12], mentioned earlier, is based on the Di Blasi and Lanzetta model [23] for the AWL calculation, provides the gaseous yield by optimizing the composition of the volatiles and determining the composition of the solid by difference.[2] The aim of the model proposed in the current study is to tackle the problem from a different point of view. That is, once the correlations describing the composition of the torrefied solid and the anhydric weight loss are established, the composition of the torrefaction gas that closes the balance may be obtained. The reasons underlying this choice are the following:

- In torrefaction experiments, only a fraction of the condensable and permanent gases is identified and quantified while the solid residue can be quantified more accurately by simply weighing the sample. The experimental relative and absolute errors are smaller when measuring a solid residue and its composition than when identifying components of a gaseous mixture. There are many studies reporting the composition of the solid as a function of the torrefaction conditions and the anhydric weight loss, but very few reporting the corresponding and detailed gas compositions (Prins et al. [13] and Nocquet [8,21]).
- The yield and elemental composition (C, H, O, N) of the solid product are the model results that require the highest accuracy as the solid is generally going to be further converted in the process. A typical value for the solid yield of torrefaction is around 90% in heating value, and 70–80% in mass.
- Torrefaction gases generally contain only about 10% of the initial heating value of biomass. In the context of this study, the gases produced during torrefaction are burnt to generate heat, therefore the main aim is to estimate their heating value rather than model their specific composition.

The model proposed in this study is structured in three sub-models, as presented in Fig. 3. The first sub-model is the anhydric weight loss model (Section 4.1). The second one is the torrefied solid composition model which describes the carbon, hydrogen, oxygen, and nitrogen content of the solid product of torrefaction as a function of the AWL (Section 4.2). The third one determines the corresponding gas composition (Section 4.3). Experimental data are generally generated on a single sample torrefied in a batch reactor. For the purpose of this study we assume that in a continuous reactor the produced gas at any time is the same as the integrated gas produced in the batch system. The model, at this point, is considered as independent from the reactor design but it is assumed that it is possible to take into account the technology by appropriately calibrating the model parameters.

### 4.1. Anhydric weight loss model

Different models exist in the literature that describe the kinetics of torrefaction [25,26]. The model used here was first introduced by Di-Blasi and Lanzetta [23] to study the kinetics of xylan degradation under inert atmosphere. It consists in a two step reaction model, consistent with the experimental observation of two stages during torrefaction. This model was first adopted by Prins et al. [14] to describe the weight loss kinetics of willow during torrefaction and it is now widely used. Nocquet et al. [24] used the same model to

---

[1] In the experimental set-up used by Nocquet [8], TORNADE, the solid product yield and composition are measured only at the end of each run, that is, after 180 min of torrefaction at a given temperature. Further calculations are therefore required for the representation of the solid composition as a function of the AWL on the ternary diagram. The AWL is calculated using the model by Di Blasi and Lanzetta [23] with parameters obtained by Nocquet et al. [24] (as will be further explained in Section 4.1). The composition of the torrefied solid is assumed to vary linearly with the AWL (as will be justified in Section 4.2).

[2] Bates and Ghoniem [12] optimizes the composition of $V_1$ and $V_2$ (see Fig. 4) on the data made available by Prins et al. [13,14] and assumes these compositions are constant. The composition of the torrefied solid is then determined by difference between the composition of the raw biomass and that of the volatiles.

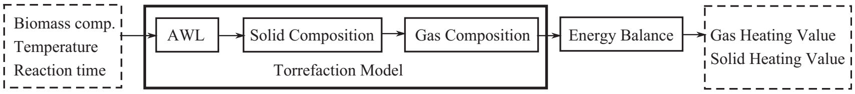

**Fig. 3.** Structure of the proposed torrefaction model.

describe beech wood torrefaction, and Shang [27] to describe wheat straw torrefaction.

In this model the initial solid A is decomposed into a volatile fraction $V_1$, reaction rate $k_{V1}$ and in an intermediate solid B, reaction rate $k_1$. B is then decomposed in a volatile fraction $V_2$, reaction rate $k_{V2}$, and a solid C, reaction rate $k_2$. The reaction mechanism is presented in Fig. 4.

The Di Blasi and Lanzetta model can thus be expressed as a system of differential equations in the form of:

$$\frac{dA}{\partial t} = -(k_1 + k_{V1})\cdot A \tag{1}$$

$$\frac{dB}{\partial t} = k_1\cdot A - (k_2 + k_{V2})\cdot B \tag{2}$$

$$\frac{dC}{\partial t} = k_2\cdot B \tag{3}$$

$$\frac{dV1}{\partial t} = k_{V1}\cdot A \tag{4}$$

$$\frac{dV2}{\partial t} = k_{V2}\cdot B \tag{5}$$

where the reaction rates, $k$, may be expressed in the form of Arrhenius equations:

$$k_i = k_{0i}\cdot e^{-\frac{E_{Ai}}{RT}} \tag{6}$$

The solid product of torrefaction can be described as the sum of solid A, B, and C. In the simplified case where thermal history is neglected and temperature is considered constant, the system of equations can be analytically solved. The solid residue $(M(t) = A + B + C)$ can be expressed as reported by Prins et al. [14]:

$$\frac{M(t)}{M_0} = \left(1 + \left[\frac{k_1K_1 - k_1k_2}{K_1(K_2 - K_1)}\right]\right)e^{-K_1t} + \left[\frac{-k_1K_2 + k_1k_2}{K_2(K_2 - K_1)}\right]e^{-K_2t} + \frac{k_1k_2}{K_1K_2} \tag{7}$$

where:

$$K_1 = k_1 + k_{V1} \tag{8}$$

$$K_2 = k_2 + k_{V2} \tag{9}$$

The Di Blasi and Lanzetta model does not provide information on the composition of the solid nor the volatiles, but it allows to calculate the AWL as a function of temperature and time. Table 1 reports sets of the eight parameters of the Di Blasi and Lanzetta model. The parameters refer to willow by Prins et al. [14], beech by Nocquet et al. [24] and wheat straw by Shang et al. [27]. Other sets of parameters can be found in the study by Repellin et al. [28].

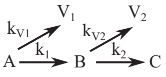

**Fig. 4.** Two step model by Di-Blasi and Lanzetta [23].

**Table 1**
Kinetic parameters.

| | Beech [24] | Willow [14] | Wheat [27] |
|---|---|---|---|
| $k_{01}$[1/s] | $1.951\cdot 10^3$ | $2.48\cdot 10^4$ | $3.48\cdot 10^3$ |
| $E_{A1}$[J/mol] | 61,780 | 75,976 | 70,999 |
| $k_{0V1}$[1/s] | $7.259\cdot 10^6$ | $3.23\cdot 10^7$ | $3.91\cdot 10^{10}$ |
| $E_{AV1}$[J/mol] | 1,076,005 | 114,214 | 139,460 |
| $k_{02}$[1/s] | $4.147\cdot 10^1$ | $1.1\cdot 10^{10}$ | $4.34\cdot 10^3$ |
| $E_{A2}$[J/mol] | 62,550 | 151,711 | 76,566 |
| $k_{0V2}$[1/s] | $2.527\cdot 10^6$ | $1.59\cdot 10^{10}$ | $3.48\cdot 10^7$ |
| $E_{AV2}$[J/mol] | 112,700 | 151,711 | 118,620 |

Hereafter the parameters determined by Nocquet et al. [24], unless otherwise specified, will be used.

### 4.2. Solid composition model

Experimental data from the literature and from previous studies carried out at CEA Grenoble was analysed in order to understand the change in composition of the torrefied solid as a function of the anhydric weight loss. The presence of ashes in raw and torrefied biomass has been neglected for simplicity. This assumption seems reasonable as ash generally accounts for 1% in wood (and up to 5–10% for straw) [29].

Fig. 5 presents data by Bridgeman et al. together with data by Prins et al. [5,17] plotted on the same graph with data by Nocquet [8,21] and other data available at CEA Grenoble, for willow, beech, and pine [30,31]. The plot shows the change in elemental composition (on a dry-ash free basis) of the torrefied solid, T00 (torrefied biomass with 0% moisture), over the composition of raw biomass, B00 (biomass with 0% moisture), as a function of the anhydric weight loss. Although the data are obtained from various initial biomass types, experimental set-ups, and conditions, it is possible to infer a linear trend for carbon and hydrogen relative concentrations.

Fig. 6 shows only the data relative to the torrefaction experiments carried out by Nocquet [8], after 180 min and at different

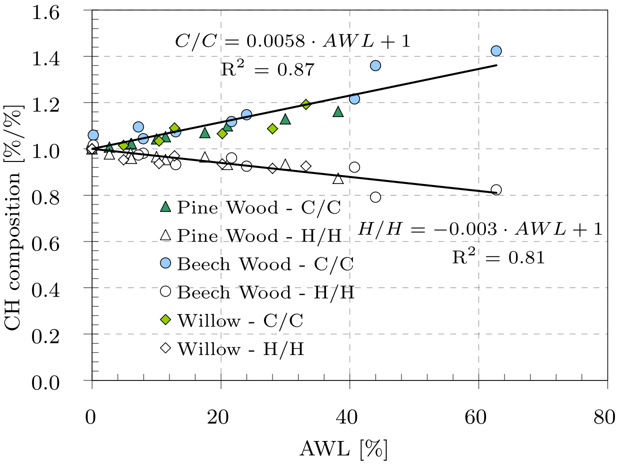

**Fig. 5.** Experimental data and linear regressions for the C and H compositions as a function of the anhydric weight loss. The data are from CEA Grenoble and the work by Bridgeman et al. and Prins et al. [5,17].

torrefaction temperatures. In this case the data are relative to the same type of biomass (beech wood), experimental set-up (TORNADE) and measurement methods. Because this data-set is the most consistent, even though a limited number of values is available, the proposed torrefaction model is based on the coefficient determined from Nocquet's [8,21] experimental results.

Solid composition may then be expressed by Equations (10) and (11). The elemental composition is intended on a dry ash-free basis, therefore oxygen can be determined by difference.

$$\frac{C\%_{T00}}{C\%_{B00}} = 1 + m_C \cdot \mathrm{AWL} \tag{10}$$

$$\frac{H\%_{T00}}{H\%_{B00}} = 1 - m_H \cdot \mathrm{AWL} \tag{11}$$

$$O\%_{T00} = 100 - C\%_{T00} - H\%_{T00} - N\%_{B00}/(100 - \mathrm{AWL}); \tag{12}$$

The parameters $m_C$ and $m_H$ may be obtained from any specific data-set. Hereafter the parameters obtained from Nocquet's experimental data [8,21], reported in Fig. 6, are used ($m_C = 0.0062$, $m_H = 0.0025$).

The simplifying assumption underlying the solid composition model presented here is that the composition of torrefied biomass depends only on the AWL, and therefore only indirectly on temperature and reaction time.

### 4.3. Gas composition model

The solid composition model (Section 4.2) describes a linear evolution of the composition of the torrefied solid as a function of the AWL. Under this assumption, the average composition of the torrefaction gases also evolves linearly, as explained in Section 3 and displayed in Fig. 2. Fig. 7 displays the composition of torrefied biomass for increasing values of anhydric weight loss, according to the model presented in Section 4.2, and the corresponding average composition of the torrefaction gases. The average composition of the torrefaction gas may in fact be determined by difference between the composition of biomass and that of the torrefied solid. As explained before the torrefaction gas is rich in oxygen and hydrogen for small AWLs and becomes closer to the composition of raw biomass as the AWL increases. Fig. 7 also displays the three most abundant chemical species generally observed during torrefaction experiments, that are water ($H_2O$), carbon dioxide ($CO_2$), and acetic acid ($C_2H_4O_2$), which combined account for about 65% of the measured gases. If the average composition estimated for the torrefaction gases falls in the triangle described on the ternary diagram by these three components, the gaseous mixture can be described as a linear combination of these gaseous species. Their concentration, as function of the AWL, can therefore be determined by simply solving a linear system of three equations and three unknowns. This approach, relying only on three gas species, is very simple and does not require any calibration on experimental values of gas composition.

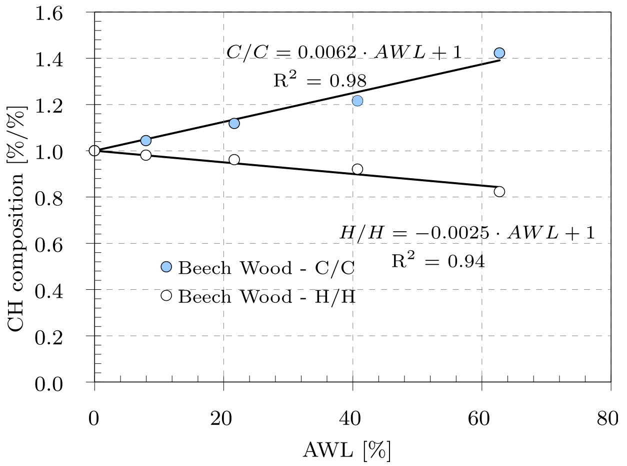

**Fig. 6.** Experimental data by Nocquet [8,21] and linear regressions for the carbon and hydrogen compositions as a function of the anhydric weight loss.

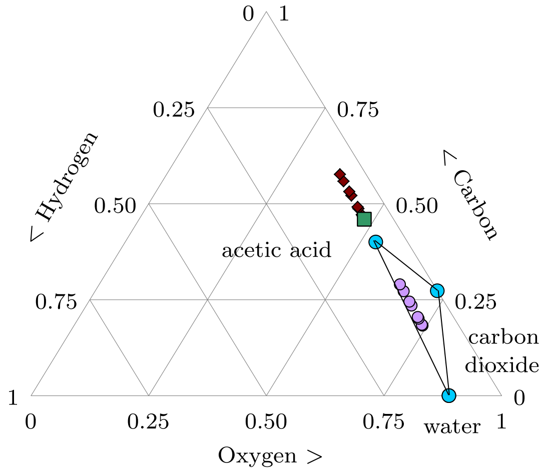

**Fig. 7.** Ternary diagram representing the carbon, hydrogen, oxygen composition of the initial biomass (green), torrefied solid (brown), average composition for the torrefaction gases (purple), and major components of the torrefaction gases (light blue). (For interpretation of the references to colour in this figure legend, the reader is referred to the web version of this article.)

The model may be calibrated with experimental results, when available, by extending the number of components used to describe the torrefaction gases. For example in Nocquet's [8,21] experimental results formaldehyde is measured in similar amounts as acetic acid. These two compounds are characterised by the same elemental mass fractions and therefore they are represented by the same point on a ternary diagram. It is therefore possible to consider a mixture of acetic acid and formaldehyde, instead of acetic acid alone and extend the number of components to four. In this case, the components considered account for about 90% of the measured gases. Hereafter this model will be referred to as the "four components model". The number of components can be further extended by defining three new vertexes on the ternary diagram as mixtures of components, by doing so it is still possible to determine the gas composition by solving a linear system of three equations in three unknowns. For example, as shown in Fig. 8, three mixtures may be defined in order to extend the gas composition from three to seven components. Mix 1 is represented by a mixture of carbon dioxide and carbon monoxide, which means that the final composition of Mix 1 is represented by a point of the line connecting the composition of carbon dioxide and carbon monoxide. Mix 2 is represented by a mixture of acetic acid and formaldehyde (both represented on the same point in the ternary diagram), and furfural. Mix 3 is represented as a mixture of water and methanol. Just for illustration purposes the ratios of the different components in the three mixtures have been optimized on eight experimental points obtained by Nocquet [8,21] at 250 °C and for different AWL, resulting in the compositions indicated by the red circles (in web version) in Fig. 8. These three new vertexes can then be used to describe the composition of the torrefaction gases, just like in the three components model described before. Hereafter this model is referred to as the "seven components model". The ratios of species

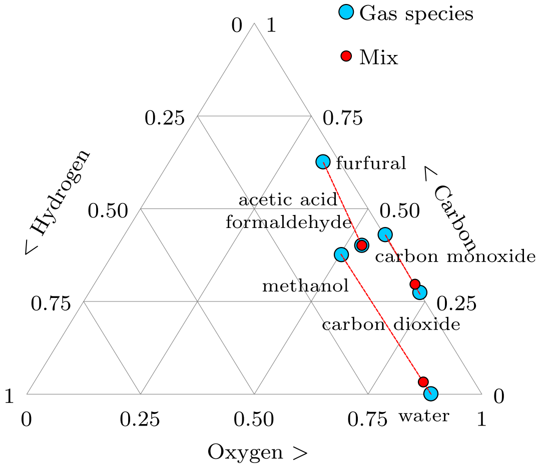

**Fig. 8.** Ternary diagram for the “seven components model”.

in the different mixtures could be defined as a function of the operating conditions. Here, for simplicity and for a first approximation, they are considered constant. The comparison with the experimental results is reported in Section 4.5. Unless otherwise specified the reference model remains the “three components model” outlined earlier.

### 4.4. Energy balance

The HHV (higher heating value) (and therefore the LHV (lower heating value)) of biomass and torrefied solid can be calculated, from their elemental composition, using the correlation by Boie [32], Equation (13). The average absolute error on the HHV of biomass fuels determined using Boie's correlation is, according to Sheng and Azevedo [33], of 3.5% (about 560 J/g). For comparison, the CEN (European Committee for Standardization) bomb calorimeter standards, for HHV measures, specify a reproducibility limit of 300 J/g [34], which represents about 1.5% of the HHV.

$$\mathrm{HHV[kJ/kg]} = 351.70\cdot \mathrm{C} + 1162.49\cdot \mathrm{H} + 104.67\cdot \mathrm{S} - 110.95\cdot \mathrm{O} + 62.80\cdot \mathrm{N} \tag{13}$$

where the HHV is on a dry basis and C, H, O, and N are the mass percentages of carbon, hydrogen, oxygen, and nitrogen also on a dry basis. The *standard enthalpy of formation* (at the reference temperature of 298 K) of biomass and the torrefied solid $\Delta_f H^\circ$ is obtained from the molar $\tilde{HHV}$ (in kJ/mol), as reported in Equation (14),[3] while their sensible heat at a given temperature can be estimated using the correlation for the heat capacity ($c_p$) of biomass proposed by Kollmann [35], Equation (15).

$$\Delta_f H^\circ_{\mathrm{CH}_x\mathrm{O}_y\mathrm{N}_z}[\mathrm{kJ/mol}] = H\tilde{H}V + \left(\frac{x}{2}\cdot\Delta_f H^\circ_{\mathrm{H_2O}_l} + \Delta_f H^\circ_{\mathrm{CO_2}} + \frac{z}{2}\cdot\Delta_f H^\circ_{\mathrm{N_2}} - \left(1+\frac{x}{4}-\frac{y}{2}\right)\cdot\Delta_f H^\circ_{\mathrm{O_2}}\right) \tag{14}$$

$$c_p[\mathrm{kJ/kgK}] = 0.00486\cdot T - 0.21293 \tag{15}$$

where $x$, $y$, $z$ are the elemental molar composition of biomass or torrefied biomass referred to 1 mol of carbon and $T$ is the temperature in Kelvin. $\Delta_f H^\circ_{N_2}$ and $\Delta_f H^\circ_{O_2}$ are equal to zero and therefore the last two terms of Equation (14) may be omitted.

Given the standard enthalpy of formation and the heat capacities of products (the torrefied solid and the produced gases) and reactants (the initial biomass), it is possible to calculate the heat of reaction of torrefaction at a given temperature. The heat of reaction of torrefaction has been measured in the literature in several studies, but its value varies as do the assumptions and the methods used for its estimation. van der Stelt [36] reports heats of reaction for the torrefaction of beech wood in the range between 1500 J/g (endothermic) and −1200 J/g (exothermic), Ohliger et al. [37] measure heat of reaction in the range of −199 J/g to 148 J/g. Bergman [1] show there is an endothermic and an exothermic phase during torrefaction and the overall heat of reaction can be positive or negative but, in terms of the overall energy balance, accounts for less than ±1% of the biomass energy input [1].

The model presented in this study, considering for example the biomass composition reported in Section 5, with an AWL of 0.2 at 250 °C, yields a heat of reaction of about −170 J/g. This exothermic heat of reaction needs to be completed with the sensible heat stored in biomass between 25 and 250 °C, which is of about +400 J/g, in order to estimate the overall heat of reaction of torrefaction. The complete heat of reaction of torrefaction, starting from biomass at 25 °C, is therefore always endothermic, under classical torrefaction conditions (between 200 °C and 300 °C), and in the present example results in +230 J/g.

### 4.5. Comparison with experimental results

The aim of this comparison is to understand how the results of the model relate to the experimental data. The comparison is carried out in terms of LHV calculated from the HHV taking into consideration the heat of vaporisation of water.

The main issue in comparing the model results against experimental data lays in the fact that the gaseous products of torrefaction are inherently difficult to quantify and identify. The mass balance error is amplified when referred to the gaseous yield. In a typical torrefaction experiment it may reach 10–40% of the AWL. As explained earlier, the proposed model is based on the solid elemental composition, while in terms of modelling of torrefaction gases, its scope is to estimate their heating value rather than model their composition. This is why the validation against experimental data is carried in terms of heating value, and not directly on the measured species present in the torrefaction gases. The comparison is carried out by affecting the *missing* carbon, hydrogen, and oxygen to the gas. The *missing* composition is obtained by difference between the composition of the initial biomass and the composition of the computed torrefied solid and measured gases. Its heating value is computed using Boie's correlation [32], Equation (13). Boie's correlation is generally used to estimate the heating value of solid and hydrocarbon fuels, when applied to torrefaction gases, such as methanol, furfural, formic acid, acetic acid and formaldehyde, it yields an error ranging from −15 to +20%. In the figures hereafter the following nomenclature is used:

- **LHV_T00 Boie**: LHV determined through Boie's correlation for the torrefied solid with the C–H–O–N from the model;
- **LHV_Gas estimate**: LHV computed by considering also the composition of the *missing gases* in order to close the balance (on a wet basis);
- **LHV_Gas model**: LHV obtained using the “three components model” (on a wet basis);

---

[3] For simplicity here complete combustion is assumed, the stoichiometric combustion reaction considered is $\mathrm{CH}_x\mathrm{O}_y\mathrm{N}_z + (1 + x/4 - y/2)\cdot\mathrm{O}_2 \rightleftharpoons \mathrm{CO}_2 + x/2\cdot\mathrm{H}_2\mathrm{O} + z/2\cdot\mathrm{N}_2$.

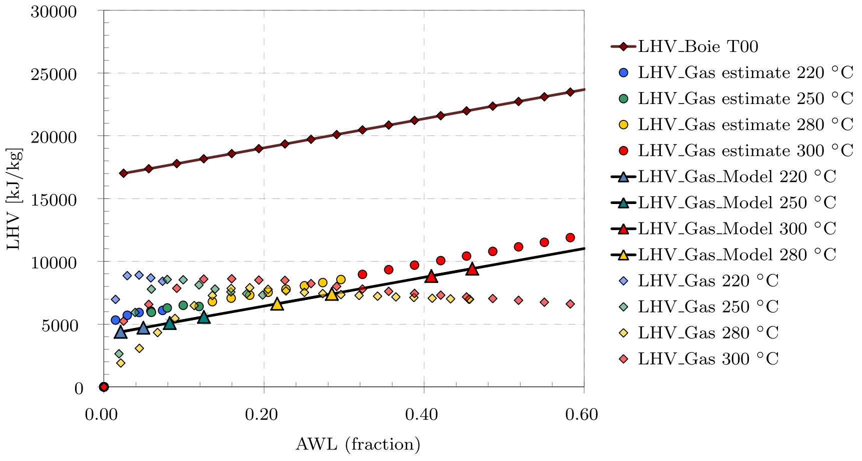

**Fig. 9.** Summary of results obtained by Nocquet [8,21] and model results.

- **LHV_Gas**: LHV computed by considering only the experimentally quantified gases produced during torrefaction and their heating values (on a wet basis);

Fig. 9 summarizes the data obtained by Nocquet [8,21] relative to torrefaction of beech wood carried out for 180 min at four different temperatures. The plot of the torrefied solid LHV as a function of the AWL is therefore obtained using the linear regression reported in Fig. 6 relative to the same set of data, and using Boie's correlation to calculate the heating value as a function of composition. The AWL is calculated as a function of temperature and residence time using the Di-Blasi and Lanzetta model and the kinetic parameters relative to beech wood, always determined by Nocquet [8] and reported in Table 1. Fig. 9 shows there is a good agreement between the estimated LHV (LHV_Gas estimate) and the modelled LHV (LHV_Gas model) of the torrefaction gases, but an important difference is displayed with the measured LHV (LHV_Gas). When considering this difference it is important to underline that (LHV_Gas) was calculated by taking into account only the gases measured by Nocquet [8] and that the total yield of the measured gases amounts to 35–100% of the calculated anhydric weight loss while the model always yields a composition that closes the balance.

As said before, the gas composition model may be extended from three to four or more components. Here, as an example, the "seven components model" previously described was calibrated on eight data points obtained by Nocquet [8,21] at the reaction temperature of 250 °C and reaction times ranging from 15 to 180 min. The results are plotted against the estimated values in Fig. 10, along the results of the "three and four components models" previously presented in Fig. 9. The "seven components model" LHV results are only slightly closer to the estimated value than the "four components" ones, and both models predict higher LHV than the "three components model". In this example, the "seven components model" describes the yield of the main gases within 20% of the experimental values when the sum of the measured gases represents over 90% of the AWL. As said before, the gas composition model may be extended from three to four or more components. Here, as an example, the "seven components model" previously described was calibrated on eight data points obtained by Nocquet [8,21] at the reaction temperature of 250 °C and reaction times ranging from 15 to 180 min. The results are plotted against the estimated values in Fig. 10, along the results of the "three and four components models" previously presented in Fig. 9. The "seven components model" LHV results are only slightly closer to the estimated value than the "four components" ones, and both models predict higher LHV than the "three components model". In this example, the "seven components model" describes the yield of the main gases within 20% of the experimental values when the sum of the measured gases represents over 90% of the AWL.

## 5. Application example

The model presented in this study is used here to represent the torrefaction step in an industrial drying and torrefaction unit. In this process the energy efficiency is usually expressed by the ratio between the energy yield in the solid product and the total energy input (feedstock and process inputs). Hereafter the energy and mass balances of drying and torrefaction of biomass are considered through flowsheet models developed using the software Vali by Belsim [7]. The drying unit is modelled as an air drying unit, using the flowsheet developed by Gassner and Maréchal [38] but not reported here in detail. The model introduced in the previous sections is used to develop the torrefaction flowsheet represented in Fig. 11. Stream B10 (biomass with 10% residual moisture) represents biomass after drying. Biomass is then heated to torrefaction temperature and torrefied. Residual moisture is completely evaporated considering, in a first approximation, a heat requirement double to that relative to the evaporation of free water (50% efficiency). The torrefied solid T00 is cooled while the torrefaction gases are combusted for heat recovery.

In this model the combustion of the torrefaction gases takes place in a **catalytic burner**, which allows recovering heat from low calorific value gas mixtures and at lower temperatures than conventional combustion, below 800 °C [39]. The model torrefaction gases of this study are $H_2O$, $CO_2$, and the only combustible component considered: $C_2H_4O_2$ (acetic acid). The minimum adiabatic flame temperature to obtain a sustainable combustion with air is set to 1100 °C. The catalytic bed temperature is set to 500 °C and a factor of 0.8 is considered to take into account heat losses in the recovery of heat. The minimum adiabatic flame temperature, the residual moisture evaporation efficiency, and the catalyst bed temperature are here considered as first approximation. Furthermore the feasibility of catalytic combustion of torrefaction gases should be validated experimentally. Process integration is carried out by considering heat integration and the recovery of the heating value of the torrefaction gases. The energy requirement of the process is satisfied by a natural gas burner when the catalytic combustion of the torrefaction gases is not sufficient. The process integration model is implemented according to the methodology

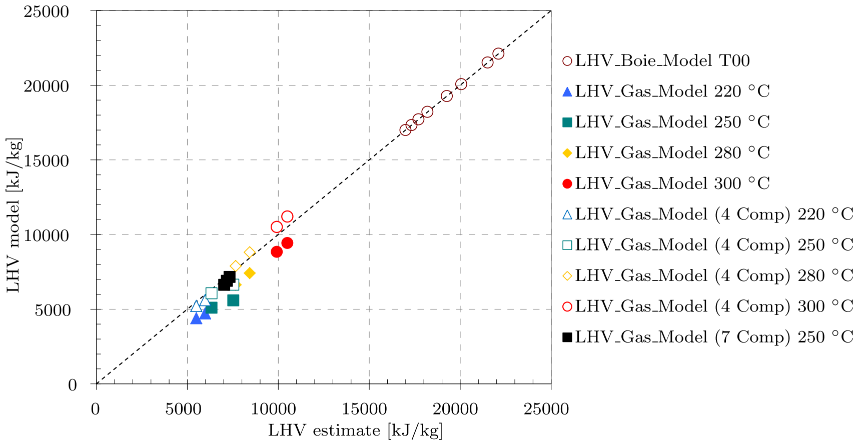

**Fig. 10.** Modelled versus estimated LHV values for the three, four and seven components models. The seven components model is calibrated using eight data points from torrefaction at 250 °C by Nocquet [8,21].

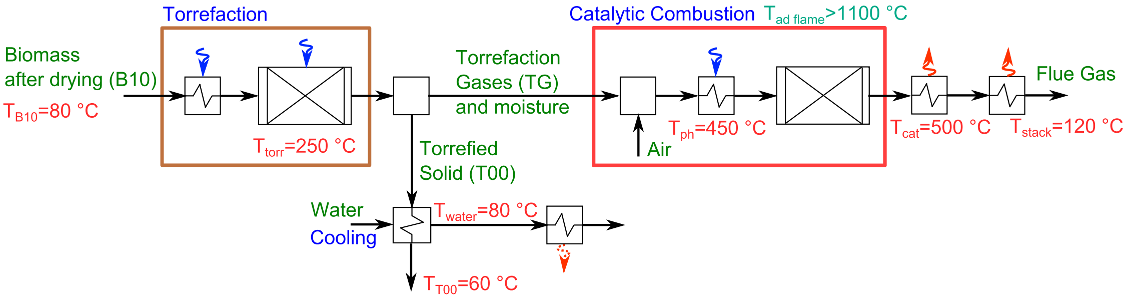

**Fig. 11.** Torrefaction flowsheet, heat requirements are represented with blue arrows (ingoing arrows) and available heat is represented with red arrows (outgoing arrows). Dotted arrows represent heat that is not considered in the process integration, non-recoverable heat. (For interpretation of the references to color in this figure legend, the reader is referred to the web version of this article.)

described by Gassner and Maréchal [40] and previously developed by Maréchal and Kalitventzeff [41,42]. The initial biomass composition is 51.5% carbon, 6.3% hydrogen, 42.0% oxygen, and 0.2% nitrogen. The torrefied solid composition, with a 20% AWL, results in 57.9% carbon, 6.0% hydrogen, 35.8% oxygen, and 0.3% nitrogen. The reference operating conditions for the proposed model are summarised in Table 2.

The heat requirement of drying and torrefaction results in 1.95 $\mathrm{MJ/kg_{B00}}$, of which 0.27 $\mathrm{MJ/kg_{B00}}$ are required for the torrefaction process alone, as reported in Table 3. The estimate of the heat of reaction of torrefaction at 250 °C reported in Section 4.4, −170 $\mathrm{J/g_{B00}}$ (−0.17 $\mathrm{MJ/kg_{B00}}$), remains small compared to the heat required for drying (~ 10%) or the biomass energy input (~ 1%). Furthermore, in the torrefaction process, the torrefaction reaction occurs together with the increase in temperature of biomass and the evaporation of its residual moisture. Therefore, from a process perspective, torrefaction is always an endothermic process, as explained in Section 4.4. Torrefaction and drying, according to the process model developed and for the operating conditions considered, display an efficiency of about 82% before process integration. Process integration allows increasing the efficiency to 90%, on a LHV basis. The high efficiency value is achieved through process integration and the use of the torrefaction gases for process heat. Furthermore, the heating value of the torrefaction gases is recovered at relatively low temperatures due to catalytic combustion. The external heat requirement is therefore reduced from 2 MJ/kg, or 0.04 $\mathrm{kg_{NG}/kg_{B00}}$ (kg of natural gas per kg of biomass), to 0.4 $\mathrm{MJ/kg_{B00}}$, or 0.008 $\mathrm{kg_{NG}/kg_{B00}}$, highlighting the importance of process integration.

## 6. Conclusions

The model proposed in this study provides a coherent description of the energy and mass balances of biomass torrefaction, in the context of process modelling and simulation. Its most relevant features may be summarised as follows:

**Table 2**
Main operating conditions.

| Section | Description | Variable | Unit | Value |
|---|---|---|---|---|
| Drying | Air inlet $T$ | $T_d$ | °C | 200 |
| | Wood Φ at inlet | $\Phi_{d,wood}$ | % | 35 |
| | Wood Φ at outlet | $\Phi_{d,wood}$ | % | 10 |
| Torrefaction | Torrefaction $T$ | $T_{torr}$ | °C | 250 |
| | Anhydric weight loss[a] | AWL | – | 0.2 |
| | Cat. comb. preheating | $T_{ph}$ | °C | 450 |
| | Cat. comb. | $T_{cat}$ | °C | 500 |
| | Stack temperature | $T_{stack}$ | °C | 120 |
| Heat integration[b] | Approach temperature, phase change | $\Delta T_{min,lv}/2$ | °C | 2 |
| | Approach temperature, liquid | $\Delta T_{min,liquid}/2$ | °C | 4 |
| | Approach temperature, gas | $\Delta T_{min,gas}/2$ | °C | 8 |
| | Approach temperature, reactor | $\Delta T_{min,reactor}/2$ | °C | 25 |

[a] The AWL is here considered as a parameter, reaction time and temperature may be considered instead by using the Di Blasi and Lanzetta model [23] as presented in Section 4.1.

[b] The temperature of each stream is corrected by the minimum approach temperature in order to take into account different heat transfer coefficients [40].

**Table 3**
Summary of mass and energy balance for the drying and torrefaction processes.

| | |
|---|---|
| $\dot{m}_{\mathrm{B00}}$ | 1.00 kg/s |
| $\mathrm{LHV}_{\mathrm{B00}}$ | 19.41 MJ/kg |
| **Drying** | |
| $\dot{m}_{\mathrm{B35}}$ | 1.54 kg/s |
| $\dot{m}_{\mathrm{B10}}$ | 1.11 kg/s |
| *Heat requirement* | 1.68 $\mathrm{MW_{th}}$ |
| **Torrefaction** | |
| $\dot{m}_{\mathrm{T00}}$ | 0.80 kg/s |
| $\mathrm{LHV}_{\mathrm{T00}}$ | 22.05 MJ/kg |
| $\dot{m}_{\mathrm{TG}}$[a] | 0.20 kg/s |
| $\mathrm{LHV}_{\mathrm{TG}}$[a] | 7.02 MJ/kg |
| Heat requirement[b] | 0.27 $\mathrm{MW_{th}}$ |

[a] In the torrefaction gases the residual moisture is not included. Including it results in an LHV of 3.64 MJ/kg and a mass flow of 0.31 kg/s.

[b] Includes the sensible heat of biomass from drying to torrefaction temperature, the evaporation of residual moisture and torrefaction.

- the calibration is carried out on the solid yield and composition. These values are determined with the smallest experimental error and are generally available in the literature;
- as a consequence, the description of the solid yield and its composition are the most accurate;
- the gas yield may be represented by three species and if experimental results are available there is the possibility to extend the calibration to the gases and therefore the number of components;
- the C–H–O balance is closed and the C–H–O composition of the gas is reasonably predicted;
- the model is simple and of fast resolution: once it is calibrated it consists of a system of linear equations;

The results of the model are compared with experimental results, in terms of LHV, leading to the following conclusions:

- The debate of exo- or endothermicity of the torrefaction reaction is not relevant in the field of process integration because the torrefaction process is always endothermic when considering the sensible heat and the heat of reaction in a steady state regime. Nevertheless, the debate remains important when considering torrefaction at the particle scale and in a transient regime, as this may have consequence for process control;
- The heating values of the torrefaction gases can be estimated with an uncertainty of ±50%. The main sources of error in the comparison are due to: the error associated to the gas measurements, the difference between estimated AWL and the total amount of identified gases, and the difficulty in identifying all measured gases. The high uncertainty underlines the importance of further experimental investigation of torrefaction, especially in terms of the evaluation of the gaseous yields.

As an example of an application for the developed model a flowsheet for the torrefaction process is presented in detail and implemented in the wider context of biomass thermo-chemical pretreatment, consisting in drying and torrefaction. The mass and energy balances are computed and the importance of process integration is highlighted by considering heat integration and the recovery of the heating value of the torrefaction gases which allows increasing the efficiency of the process from 82% to 90%, on a LHV basis.

This work represents the basis for a future optimisation of biomass pretreatment and its coupling with the thermo-chemical conversion of biomass. It will allow therefore a better understanding of the trade-offs concerning optimal operating parameters in particular in terms of drying level (residual moisture content) and anhydric weight loss for the improvement of pretreatment (torrefaction and drying) and overall process efficiency.

## Acknowledgements

Acknowledgements are due to Timothé Nocquet, Thierry Melkior and Thierry Chataing for providing the data used in this study and helpful discussion.

## References

[1] Bergman P. Torrefaction for biomass co-firing in existing coal-fired power station. Technical Report, ECN Biomass; 2005.
[2] Trifonova R, Babini V, Postma J, Ketelaars J, van Elsas J. Colonization of torrefied grass fibers by plant-beneficial microorganisms. Appl Soil Ecol 2009;41:98–106.
[3] Bridgeman T, Jones J, Williams A, Waldron D. An investigation of the grindability of two torrefied energy crops. Fuel 2010;89:3911–8.
[4] Phanphanich M, Mani S. Impact of torrefaction on the grindability and fuel characteristics of forest biomass. Bioresour Technol 2011;102:1246–53.
[5] Bridgeman T, Jones J, Shield I, Williams P. Torrefaction of reed canary grass, wheat straw and willow to enhance solid fuel qualities and combustion properties. Fuel 2008;87:844–56.
[6] Dhungana A, Basu P, Dutta A. Effects of reactor design on the torrefaction of biomass. J Energy Resour Technol 2012;134:041801.
[7] Belsim SA, Belsim Vali. 2013. URL: www.belsim.com.
[8] Nocquet T. Torréfaction du bois et de ses constituants: expériences et modélisation des rendements en matières volatiles. Ph.D. thesis. Institut National Polytechnique de Toulouse (INP Toulouse); 2012. URL, http://ethesis.inp-toulouse.fr/archive/00002140/01/nocquet.pdf.
[9] Tumuluru JS, Sokhansanj Shahab, Wright CT, Kremer T. GC analysis of volatiles and other products from biomass torrefaction process. In: Mohd Mustafa Ali, editor. Advanced gas chromatography – progress in agricultural, biomedical and industrial applications; 2012. ISBN: 978-953-51-0298-4. InTech, Available from: http://www.intechopen.com/books/advanced-gas-chromatography-progress-in-agricultural-biomedical-and-industrial-applications/gc-analysis-of-volatiles-and-other-products-from-biomass-torrefaction-process.
[10] Hall W. Assessment of carbon dioxide emissions reductions achievable by using torrefaction. J Energy Inst 2012;85:103–13.
[11] Medic D, Darr M, Shah A, Potter B, Zimmerman J. Effects of torrefaction process parameters on biomass feedstock upgrading. Fuel 2012;91:147–54.
[12] Bates RB, Ghoniem AF. Biomass torrefaction: modeling of volatile and solid product evolution kinetics. Bioresour Technol 2012;124:460–9.
[13] Prins MJ, Ptasinski KJ, Janssen FJ. Torrefaction of wood: part 2. Analysis of products. J Anal Appl Pyrolysis 2006a;77:35–40.
[14] Prins MJ, Ptasinski KJ, Janssen FJ. Torrefaction of wood: part 1. Weight loss kinetics. J Anal Appl Pyrolysis 2006b;77:28–34.
[15] Chew J, Doshi V. Recent advances in biomass pretreatment torrefaction fundamentals and technology. Renew Sustain Energy Rev 2011;15:4212–22.
[16] Cairns EJ, Tevebaugh AD. CHO Gas phase compositions in equilibrium with carbon, and carbon deposition boundaries at one atmosphere. J Chem Eng Data 1964;9:453–62.
[17] Prins MJ, Ptasinski KJ, Janssen FJ. More efficient biomass gasification via torrefaction. Energy 2006;31:3458–70.
[18] Ptasinski KJ, Prins MJ, Pierik A. Exergetic evaluation of biomass gasification. Energy 2007;32:568–74.
[19] Tay DHS, Ng DKS, Kheireddine H, El-Halwagi MM. Synthesis of an integrated biorefinery via the CHO ternary diagram. Clean Technol Environ Policy 2011;13:567–79.
[20] Chen L, Dupont C, Salvador S, Grateau M, Boissonnet G, Schweich D. Experimental study on fast pyrolysis of free-falling millimetric biomass particles between 800 °C and 1000 °C. Fuel 2013;106:61–6.
[21] Nocquet T, Dupont C, Commandré J-M, Grateau M, Thiéry S, Salvador S. Volatile species release during torrefaction of biomass and its constituents part I: experimental study. Energy; 2014:1–8 [in press]. Available here: http://www.sciencedirect.com/science/article/pii/S0360544214001959.
[22] Nocquet T, Dupont C, Commandré J-M, Grateau M, Thiéry S, Salvador S. Volatile species release during torrefaction of biomass and its constituents part II: modelling study. Submitted to Energy; 2013.
[23] Di Blasi C, Lanzetta M. Intrinsic kinetics of isothermal xylan degradation in inert atmosphere. J Anal Appl Pyrolysis 1997;40–41:287–303.
[24] Nocquet T, Dupont C, Commandré J-M, Boachon C, Soudais Y, Salvador S. Study on mass loss and gas release during torrefaction of woody biomass ant its constituents for injection in entrained flow gasifier. In: 3rd International Congress on Green Process Engineering, Kuala-Lumpur; 2011.
[25] Di Blasi C. Modeling chemical and physical processes of wood and biomass pyrolysis. Prog Energy Combust Sci 2008;34:47–90.
[26] van der Stelt M, Gerhauser H, Kiel J, Ptasinski K. Biomass upgrading by torrefaction for the production of biofuels: a review. Biomass Bioenergy 2011;35:3748–62.

[27] Shang L, Ahrenfeldt J, Holm JK, Barsberg S r, Zhang R-z, Luo Y-h, et al. Intrinsic kinetics and devolatilization of wheat straw during torrefaction. J Anal Appl Pyrolysis 2013;100:145–52.

[28] Repellin V, Govin A, Rolland M, Guyonnet R. Modelling anhydrous weight loss of wood chips during torrefaction in a pilot kiln. Biomass Bioenergy 2010;34:602–9.

[29] Dupont C, Rougé S, Berthelot A, Da Silva Perez D, Graffin A, Labalette F, et al. Bioenergy II: suitability of Wood chips and various biomass types for use in plant of BtL production by gasification. Int J Chem React Eng 2010;8.

[30] Marty C. Adaptation et optimisation à la torréfaction de la technologie four à plateaux développée par la société CMI. Technical Report. France: Univeristé Joseph Fourier de Grenoble; 2011.

[31] Commandré J-M, Rousset P, Lesueur G, Leboeuf A, Chafchaouni L. Torrefaction of biomass : influence of operating conditions on products. In: WasteEng10: 3rd International Conference on Engineering for Waste and Biomass Valorisation, Beijing; 2010.

[32] Boie W. Fuel technology calculations. Energietechnik 1953;3:309–16.

[33] Sheng C, Azevedo J. Estimating the higher heating value of biomass fuels from basic analysis data. Biomass Bioenergy 2005;28:499–507.

[34] European Committee for Standardization, EN 14918:2009. Solid biofuels – determination of calorific value; 2009.

[35] Kollman F. Technologie des Holzes und der Holzwerkstoffe. Heidelberg: Springer; 1982.

[36] van der Stelt M. Chemistry and reaction kinetics of biowaste torrefaction. Ph.D. thesis. Technical University of Eindhoven (TU/e); 2010.

[37] Ohliger A, Förster M, Kneer R. Torrefaction of beechwood: a parametric study including heat of reaction and grindability. Fuel 2013;104:607–13.

[38] Gassner M, Maréchal F. Thermo-economic process model for thermochemical production of synthetic natural Gas (SNG) from lignocellulosic biomass. Biomass Bioenergy 2009;33:1587–604.

[39] Geus JW, van Giezen JC. Monoliths in catalytic oxidation. Catal Today 1999;47:169–80.

[40] Gassner M, Maréchal F. Methodology for the optimal thermo-economic, multi-objective design of thermochemical fuel production from biomass. Comput Chem Eng 2009;33:769–81.

[41] Maréchal F, Kalitventzeff B. Process integration: selection of the optimal utility system. Comput Chem Eng 1998;22:S149–56.

[42] Maréchal F, Kalitventzeff B. Targeting the minimum cost of energy requirements: a new graphical technique for evaluating the integration of utility systems. Comput Chem Eng 1996;20:225–30.